Simultaneous measurement of duskside subauroral irregularities from the CUTLASS Finland radar and EISCAT UHF system

K. Hosokawa,[1] M. Sugino,[2] M. Lester,[3] N. Sato,[4] A. S. Yukimatu,[4] and T. Iyemori[5]

Received 28 March 2002; revised 13 May 2002; accepted 4 June 2002; published 19 December 2002.

[1] Dusk scatter event (DUSE) (first reported by *Ruohoniemi et al.* [1988]) is one of the most reproducible features among the SuperDARN radar backscatter within the subauroral ionosphere. *Hosokawa et al.* [2001] analyzed the scattering occurrence percentage of the Northern Hemisphere SuperDARN radars in a statistical fashion and pointed out that the region where the DUSE appears has a close relationship with the duskside end of the midlatitude trough in longitudinal direction. They proposed a model explaining the generation of the DUSE which employs a Sunward density gradient at the duskside edge of the trough and an ambient poleward electric field. In order to confirm the model proposed by *Hosokawa et al.* [2001], we have investigated two DUSE events which had been observed by the CUTLASS Finland radar and the EISCAT UHF system simultaneously. Consequently, when the CUTLASS Finland radar observed the DUSE, a Sunward directed density gradient was observed by the EISCAT in the vicinity of the DUSE. After the passage of the DUSE the EISCAT observed an ion temperature enhancement which suggested that the EISCAT entered the trough through its duskside edge. These observational facts suggest that the geometry of the parameters around the DUSE is quite consistent with the model proposed by *Hosokawa et al.* [2001]. In addition, the EISCAT observed an enhancement of the poleward electric field around the DUSE, and a signature of the substorm was identified by the ground magnetometer on the nightside. We suggest generation mechanisms of the trough responsible for the DUSE during substorm conditions in terms of the role of the enhanced subauroral electric field and discuss a relationship between the DUSE and the other substorm-related phenomena. *INDEX TERMS:* 2439 Ionosphere: Ionospheric irregularities; 2443 Ionosphere: Midlatitude ionosphere; 2463 Ionosphere: Plasma convection; 2467 Ionosphere: Plasma temperature and density; 2788 Magnetospheric Physics: Storms and substorms; *KEYWORDS:* ionospheric irregularities, subauroral ionosphere, midlatitude trough, storm and substorm

Citation: Hosokawa, K., M. Sugino, M. Lester, N. Sato, A. S. Yukimatu, and T. Iyemori, Simultaneous measurement of duskside subauroral irregularities from the CUTLASS Finland radar and EISCAT UHF system, *J. Geophys. Res.*, *107*(A12), 1457, doi:10.1029/2002JA009416, 2002.

1. Introduction

[2] Ionospheric field aligned plasma irregularities (FAIs) are structures in plasma density which have been produced by plasma instability processes from initial perturbations [*Fejer and Kelley*, 1980; *Keskinen and Ossakow*, 1983]. The subauroral F region ionosphere is one of the active sources of FAIs and therefore a good target for coherent scatter radars (as reviewed by, for example, *Tsunoda* [1988]). *Ruohoniemi et al.* [1988] had earlier focused on the radar echoes observed by the Goose Bay HF radar which forms part of the Super Dual Auroral Radar Network (SuperDARN) [*Greenwald et al.*, 1995] in the subauroral F region and identified a distinctive backscatter feature known as the dusk scatter event (DUSE). They investigated the DUSE during quiet geomagnetic conditions over a period of 5 months centered on winter solstice and reported that it appears when the solar zenith angle is near 95° and the source of these backscatters lies in the magnetic latitudes equatorward of the auroral oval (i.e., near the poleward edge of the midlatitude trough; for the detail of the midlatitude trough see the review by *Rodger et al.* [1992]). Occurrence of the DUSE is 100% during winter, which means that the DUSE is one of the most reproducible features among the SuperDARN observations. They proposed several models to explain the enhancement of FAIs in this region. However, the generation mechanism of FAIs responsible for the DUSE was still an open question and the morphological feature of the DUSE during disturbed condition was also unresolved.

[1]Department of Geophysics, Graduate School of Science, Kyoto University, Kyoto, Japan.
[2]Solar-Terrestrial Environment Laboratory, Nagoya University, Nagoya, Japan.
[3]Department of Physics and Astronomy, University of Leicester, Leicester, UK.
[4]National Institute of Polar Research, Tokyo, Japan.
[5]Data Analysis Center for Geomagnetism and Space Magnetism, Graduate School of Science, Kyoto University, Kyoto, Japan.

0148-0227/02/2002JA009416$09.00

[3] *Hosokawa et al.* [2001] extended the work of *Ruohoniemi et al.* [1988] by analyzing the scattering occurrence percentage of the Northern Hemisphere SuperDARN radars in a statistical fashion. In all months the DUSE appears within a few hours of local time on the eveningside of sunset, where the magnetic latitude is slightly lower than the equatorward edge of the auroral oval. The most significant finding is that the region where the DUSE occurs has a close relationship with the duskside end of the midlatitude trough in longitudinal direction (which is termed the Sunward edge of the trough in this paper), where the Sunward directed steep plasma density gradient exists. They also found that the signature of the DUSE appears at earlier local time during disturbed conditions compared with those during quiet conditions. *Halcrow and Nisbet* [1977] pointed out that the location of the Sunward edge of the trough is highly controlled by the solar zenith angle and the level of geomagnetic disturbance as estimated by the *Kp* index. In short, the Sunward edge of the trough is located at the region where the solar zenith angle is 95° (evening side of local sunset) during quiet conditions and it extends further into the dayside with the *Kp* index increasing. This feature is confirmed by the other observations [*Whalen*, 1987, 1989, 1994] and by the modeling work [*Sojka et al.*, 1990]. On the basis of these characteristics of the DUSE and the midlatitude trough, Hosokawa and colleagues suggested that the Sunward directed electron density gradient at the Sunward edge of the trough is a key parameter for the generation of the DUSE and then proposed a model of the DUSE generation mechanism which is based on the gradient drift instability.

[4] Figure 1 demonstrates a schematic illustration of the model proposed by *Hosokawa et al.* [2001]. The poleward and equatorward edges of the auroral oval are plotted and the gray-shaded region located just outside of the auroral oval indicates the midlatitude trough. At the Sunward edge of the trough a Sunward-directed steep density gradient exists. The model employs this Sunward plasma density gradient, the downward geomagnetic field and the ambient poleward electric field in the subauroral region (which is identical to the westward plasma drift). Assuming the DUSE is produced in gradient drift instability process, the geometry of these parameters is favorable for the growth of the initial plasma density fluctuation (see *Keskinen and Ossakow* [1983] in detail). This model is consistent with all statistical characteristics of the DUSE during both quiet and disturbed conditions. However, the SuperDARN radars can not observe electron density and plasma temperature in the vicinity of the DUSE; hence *Hosokawa et al.* [2001] could not discuss the validity of the model in detail. In order to confirm this model, we have investigated two DUSE events which had been observed by the CUTLASS Finland radar and the EISCAT UHF system simultaneously. The EISCAT mainland UHF system has a common volume with the CUTLASS Finland radar (easternmost radar of the Northern Hemisphere SuperDARN chain) and can provide background parameters of the DUSE such as the two-dimensional electric field, electron density, and plasma temperature. Using these background parameter observations, we can closely discuss the relationship between the appearance of the DUSE and the electron density gradient at the Sunward edge of the midlatitude trough.

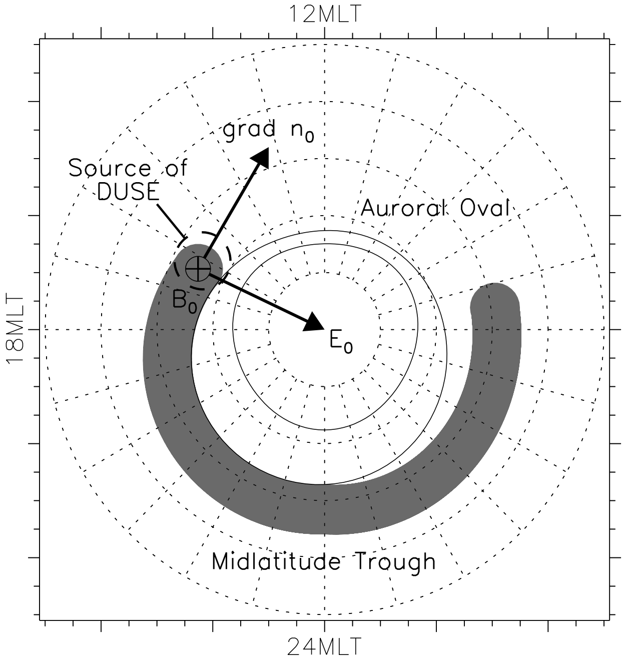

Figure 1. Schematic illustration of the model proposed by *Hosokawa et al.* [2001]. The poleward and equatorward edges of the auroral oval are plotted, and the gray-shaded region located just outside of the auroral oval indicates the midlatitude trough. Source of the DUSE is shown by the dotted circle at the duskside edge of the midlatitude trough (see the text in detail).

[5] Previous studies of the trough [*Knudsen*, 1974; *Knudsen et al.*, 1977; *Spiro et al.*, 1978] suggested that the midlatitude trough is primarily created by ordinary loss through recombination in darkened regions of stagnated plasma flow (stagnation trough theory). At subauroral latitudes the Earth corotation and auroral electric field induced convection compete, which produces region of stagnated plasma flow in the evening sector. Flux tubes containing F region plasma are confined to this stagnation region and spend many hours. The decay of ionization in these flux tubes then is thought to lead to the formation of trough. Other authors [*Evans et al.*, 1983; *Holt et al.*, 1983; *Providakes et al.*, 1989] have reported that the trough is formed by an enhanced recombination in regions of rapid subauroral plasma drift through ion-frictional heating [*Schunk et al.*, 1975] (enhanced recombination trough theory). These high-speed plasma drift signatures in the subauroral F region ionosphere could be originated from the occurrence of the substorm and might correspond to the feature known as the subauroral ion drift (SAID) [*Galperin et al.*, 1973; *Smiddy et al.*, 1977; *Anderson et al.*, 1991, 1993, 2001; *Karlsson et al.*, 1998]. As is already noted, *Hosokawa et al.* [2001] demonstrated that the local time sector where the DUSE appears extends further into the dayside with the *Kp* index increasing. This feature must be discussed in relation to the proposed formation mechanisms of the trough during disturbed conditions (i.e., under the geomagnetic substorm condition). Since the two DUSE events examined in this paper occurred during moderately disturbed conditions (*Kp* index ranges from 3 to 4-), we are able to discuss this point in terms of the

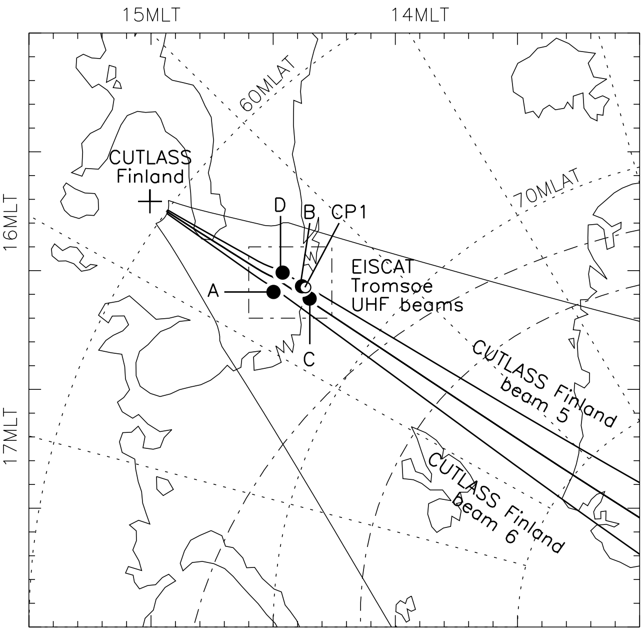

Figure 2. Map showing the location of the fields of view of the instruments used for this study in geomagnetic coordinate system(geomagnetic latitude and magnetic local time in the AACGM coordinates) at 1320 UT. Fan-shaped area indicates the field of view of the CUTLASS Finland radar. White circle depicts the tristatic position of the EISCAT CP-1 mode at 278 km altitude. Four black circles from A to D indicate the EISCAT CP-2 beam positions at 250 km altitude. Two dot-dashed lines indicate the equatorward and poleward edges of the auroral oval [*Feldstein and Starkov*, 1967] as modeled by *Holzworth and Meng* [1975] for *Kp* = 3.

trough formation mechanism during disturbed conditions and its association with the other substorm-related phenomena.

2. Experimental Arrangement

[6] This paper presents two separate intervals of simultaneous observations of subauroral plasma irregularities from the CUTLASS Finland radar and the EISCAT UHF system. This section contains a brief description of the two radar systems and the data sets therefrom. Figure 2 depicts the field of view of the Co-operative UK Twin Located Auroral Sounding System (CUTLASS) [*Milan et al.*, 1997] Finland radar mapped into the Altitude Adjusted Corrected Geomagnetic (AACGM) coordinate system (based on *Baker and Wing* [1989]) at 1320 UT. The CUTLASS Finland radar is the easternmost radar of the SuperDARN network [*Greenwald et al.*, 1995] in the Northern Hemisphere. The magnetic latitude of the Finland radar is relatively low (59.21°), which is suitable for the detection of the DUSE. The radar can operate at specific frequencies within the range 8 to 20 MHz, although the operating frequency is typically near 10 MHz, which corresponds to a wavelength of the scattering plasma irregularities of 15 m. During both intervals of this study the CUTLASS Finland radar was running in normal scan mode. The radar scans through 16 azimuthal beams in every 2 minutes, and the dwell time on each beam is typically 7 s in standard common mode operation. Each beam is separated into 75 range gates. In standard common mode these range gates are 45 km in length with a distance to the first gate of 180 km.

[7] The European Incoherent Scatter (EISCAT) radars have also been used in this work [*Rishbeth and Williams*, 1985]. The EISCAT UHF incoherent scatter radar facility, which operates at frequencies around 931 MHz, comprises three antennas, one sited at Tromsoe, Northern Norway, which combines both transmit and receive capabilities and two remote site receivers, at Kiruna in Sweden and Sodankyla in Finland. In this study we employed data from the EISCAT UHF common programs, CP-1 and CP-2 [e.g., *Rishbeth and Williams*, 1985]. Specifically, we used estimates of electron density, ion and electron temperature, and two-dimensional electric field. In the EISCAT CP-1 mode the beam from the UHF transmitter is aligned along the local F region magnetic field direction which is at an elevation of around 77° and a geographic azimuth of 182°. In CP-2, the transmitter performs a four-position scan, one position of which is field-aligned, another of which is vertical and the remaining two which are directed southeastward. The dwell time for each position of the scan is 90 s, giving a total cycle time of 6 min.

[8] The locations of the F region tristatic volume for EISCAT CP-1 and the four pointing direction of CP-2 are overplotted in Figure 2. White circle shows the position of CP-1 mode at 278 km altitude (magnetic latitude is 66.48°) and four black circles from A to D indicate the positions of CP-2 mode at 250 km altitude (magnetic latitude is 65.54°, 66.34°, 66.90°, and 65.36°, respectively). For the field-aligned UHF antenna pointing directions (CP-1 and position B of CP-2) the F region intersection volume lies within range gate 16 (corresponding radar range of 900 km) of beam 5 of the CUTLASS Finland radar field of view (see *Davies et al.* [1999] for the detail). The DUSE normally appears at the radar range of 600–1500 km in the field of view of the SuperDARN radars; hence the configuration of the CUTLASS Finland radar and EISCAT UHF system is suitable for simultaneous observation of the DUSE.

3. Observations

[9] As noted before, this paper presents two simultaneous observations of the DUSE from the CUTLASS Finland radar and the EISCAT UHF system. One occurred on 14 February 1996 (hereinafter referred as event A) and the other on 12 October 1996 (hereinafter referred as event B). In this section we first introduce these DUSE events observed by the CUTLASS Finland and background parameters obtained from the EISCAT UHF system. Next, we briefly check background conditions observed by the EISCAT during an interval when the DUSE does not appear in the field of view of the CUTLASS Finland radar for comparison. Finally, a relationship between the appearance of the DUSE and the occurrence of the geomagnetic substorm is examined using ground magnetic field variations obtained from the magnetometers located on the nightside.

3.1. CUTLASS Finland Observations

3.1.1. Event A: 14 February 1996

[10] The upper six panels of Figure 3 show the set of the maps of line-of-sight Doppler velocity illustrating the devel-

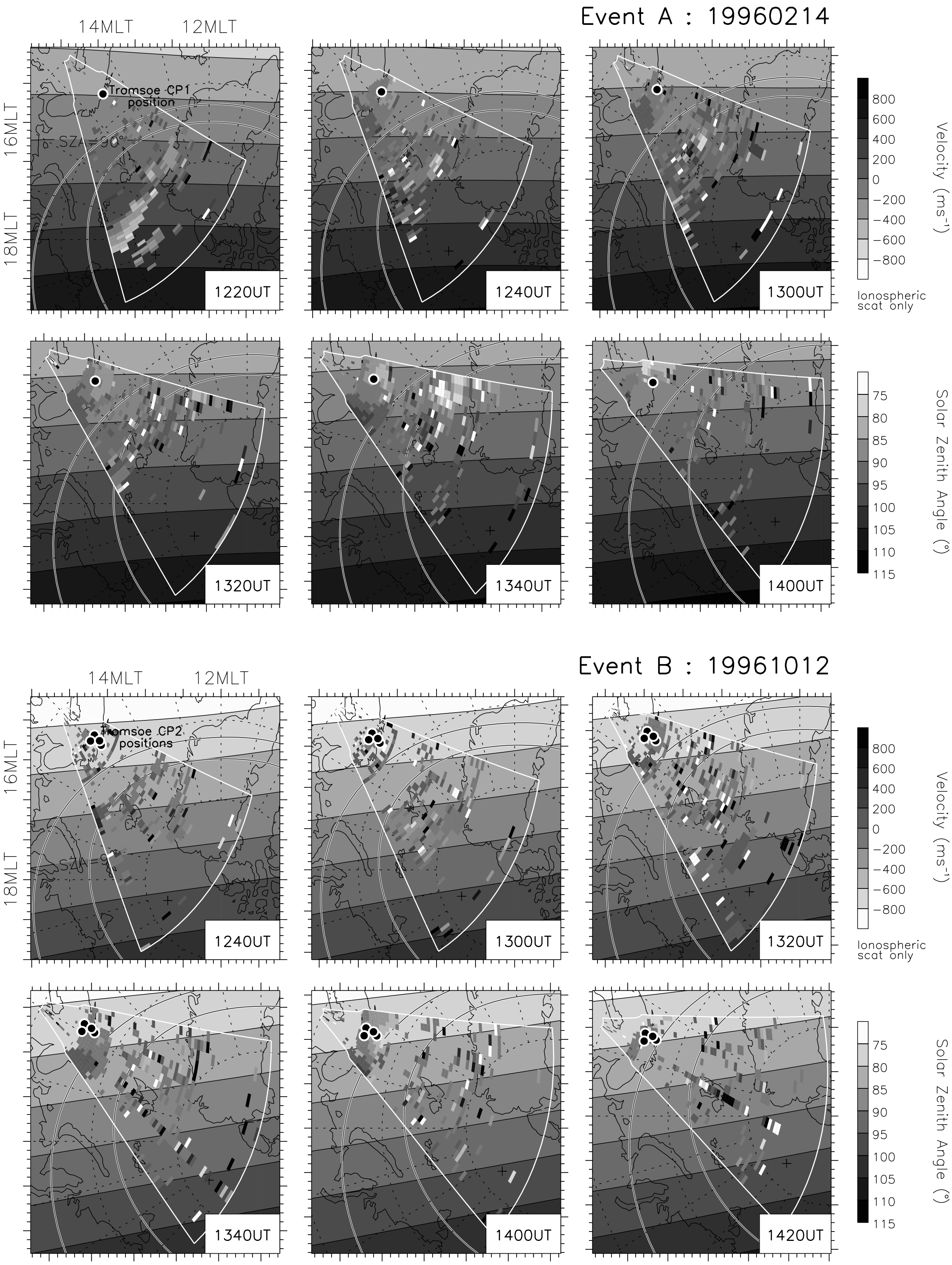
Event A : 19960214
14MLT
12MLT
16MLT
18MLT
Tromsoe CP1 position
SZA=90°
1220UT
1240UT
1300UT
1320UT
1340UT
1400UT
Velocity (ms⁻¹)
800
600
400
200
0
−200
−400
−600
−800
Ionospheric scat only
Solar Zenith Angle (°)
75
80
85
90
95
100
105
110
115
Event B : 19961012
14MLT
12MLT
16MLT
18MLT
Tromsoe CP2 positions
1240UT
1300UT
1320UT
1340UT
1400UT
1420UT

opment of the DUSE on 14 February 1996. The data are mapped into the AACGM geomagnetic latitude and MLT coordinates. The closed circle indicates the field of view of EISCAT CP-1 field aligned beam at F region altitudes. In the second map (1240 UT) the patch of backscatter emerges from near the coast of Scandinavia. Twenty minutes earlier (the first map: 1220 UT), there is no such activity in this area. These echoes are due to backscatter from FAIs in the ionosphere at radar ranges of 900–1300 km. In the Super-DARN observations the radar echoes whose range is larger than 900 km are generally defined to be due to F region scatter; hence these echoes are considered to be from F region FAIs. The fourth (1320 UT) and fifth (1340 UT) maps show that this scatter consolidates into a region that spans the entire range of radar azimuths. By the time of the last map (1400 UT) the scatter has disappeared on the eastern beams. The shifting continues until the image moves entirely off the western edge of the field of view at 1425 UT. This example illustrates the general development of the DUSE. In short, the activity turns on in the space of several minutes at dusk, develops into a latitudinally confined region extending through $\sim$1 hour in longitudinal direction, and decays by a westward movement that eventually takes it out of the radar field of view. The time from first appearance to complete departure is $\sim$115 min in this case, which is slightly longer than the typical duration of 1–1.5 hours suggested by *Ruohoniemi et al.* [1988].

[11] The poleward and equatorward edges of the Feldstein auroral oval [*Feldstein and Starkov*, 1967] as modeled by *Holzworth and Meng* [1975] for $Kp = 3$ (Kp value for the period 1200–1500 UT was 3+) are illustrated by the black on white lines. *Ruohoniemi et al.* [1988] and *Hosokawa et al.* [2001] pointed out that the source of the DUSE is closely related to the structure of the midlatitude trough. Also in this case, the DUSE appears just equatorward of the average auroral oval, which is quite consistent with the previous observations. The background gray scaled colors display the contour of solar zenith angle on the day of this event. The DUSE appears for a solar zenith angle ranging 85°–92°. *Ruohoniemi et al.* [1988] pointed out that the DUSE generally occurs when the solar zenith angle is near 95°. In this case, the solar zenith angle where the DUSE appears is smaller in comparison with the typical DUSE events. *Hosokawa et al.* [2001] indicated that the DUSE appears at earlier local times (for a smaller solar zenith angle) in magnetically disturbed conditions compared with those in quiet conditions. Since geomagnetic activity during this interval was moderately disturbed, the appearance of the DUSE for a smaller solar zenith angle is also consistent with the characteristics of the DUSE revealed by *Hosokawa et al.* [2001].

[12] Moving now to the line-of-sight Doppler velocities in Figure 3, we note that positive (negative) values represent irregularity toward (away from) the radar. Then the pattern observed at the time of the fifth panel (1340 UT) is a smooth variation from negative values (≈ -500 m s^{-1}) on the most westerly beams, through zero on the most central beams, to positive values (≈ 400 m s^{-1}) on the most easterly beams. *Ruohoniemi et al.* [1988] demonstrated that the DUSE typically exhibits low (≤ 200 m s^{-1}) line-of-sight Doppler velocities, indicative of small (≤ 50 m s^{-1}) poleward drift across L-shell contours and small (≤ 150 m s^{-1}) Sunward drift. The Doppler velocity values obtained in this event are larger than those of *Ruohoniemi et al.* [1988]. This difference could be due to the difference in the level of geomagnetic disturbance, which will be discussed in detail later. Finally, we note that width of Doppler velocity spectra is narrow (≤ 200 m s^{-1}) throughout the interval, which is also consistent with the result of *Ruohoniemi et al.* [1988].

3.1.2. Event B: 12 October 1996

[13] The lower six panels of Figure 3 show a set of the maps of line-of-sight Doppler velocity on 12 October 1996. The format is the same as the upper six panels, but in this case four solid circles indicate the fields of view of the four beam directions of the EISCAT CP-2 mode at F region altitudes. The DUSE first appears on the eastern beams in the third map (1320 UT), then intensifies and covers all radar azimuths by the time of fourth (1340 UT) and fifth (1400 UT) map, and finally moves off the western edge of the field of view (sixth map: 1420 UT). This example is also consistent with the general development and disappearance of the DUSE described by *Ruohoniemi et al.* [1988]. The poleward and equatorward edges of the Feldstein auroral oval for $Kp = 4$ (Kp value for the period 1200–1500 UT was 4-) are also shown as the black on white lines. Again, the poleward edge of the DUSE backscatter is located at equatorward edge of the auroral oval, which is consistent with both *Ruohoniemi et al.* [1988] and *Hosokawa et al.* [2001]. The Doppler velocity and spectral width observed during this interval are similar to those observed in event A.

[14] As noted before, the background gray scaled colors display the contour of solar zenith angle. The DUSE appears for a solar zenith angle ranging from 77°–83°. In this case, the solar zenith angle where the DUSE appears is further smaller than that in event A, which again is consistent with the statistical result of *Hosokawa et al.* [2001] that the DUSE appears at earlier local times as the level of magnetic disturbance increases. If we observe the DUSE at a fixed latitude, it would appear at earlier local time sector with the oval being expanded. Since field of view of the radar is fixed in this case, the effect of expanded auroral oval also could contribute to the appearance of the DUSE at lower solar zenith angles by a small degree. In this event, the time from first appearance to complete departure is $\sim$65 min, which is shorter than that in event A and at the lower end of the range identified by *Ruohoniemi et al.*

Figure 3. (opposite) Summary of the observation by the CUTLASS Finland radar for the two intervals of interest. The upper six panels show the set of the maps of the line-of-sight Doppler velocity illustrating development of the DUSE activity for event A (14 February 1996), and the lower six panels for event B (12 October1996), where motion of plasma away from the radar is negative, and toward the radar is positive. The poleward and equatorward edges of the Feldstein auroral oval [*Feldstein and Starkov*, 1967] as modeled by *Holzworth and Meng* [1975] are overplotted as $Kp = 3$ for event A and as $Kp = 4$ for event B. The background gray scaled colors display the contour of solar zenith angle. See color version of this figure at back of this issue.

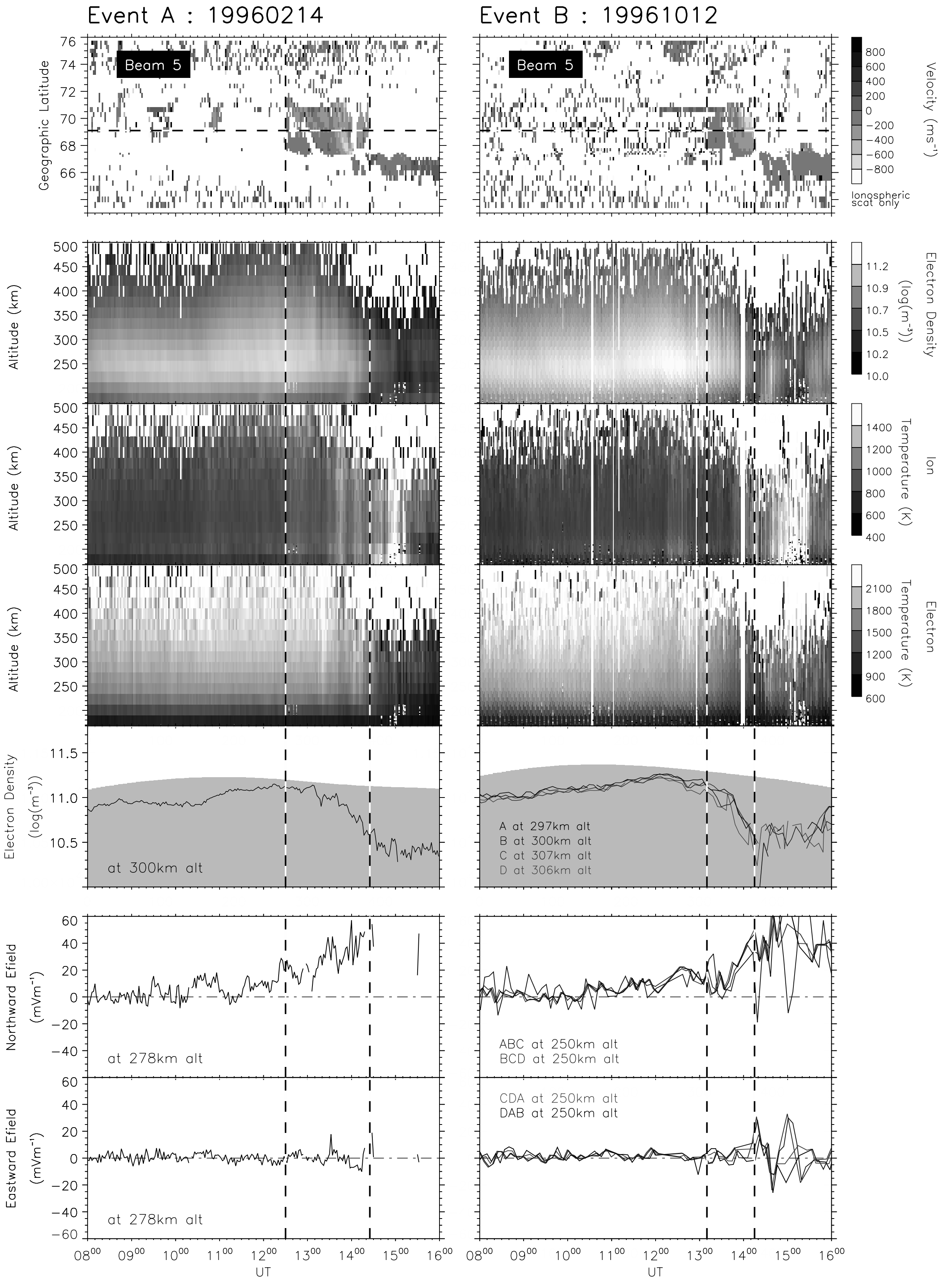
Event A : 19960214
Event B : 19961012
Beam 5
Beam 5
Geographic Latitude
Velocity (ms⁻¹)
Ionospheric scat only
Altitude (km)
Electron Density (log(m⁻³))
Ion Temperature (K)
Electron Temperature (K)
Electron Density (log(m⁻³))
at 300km alt
A at 297km alt
B at 300km alt
C at 307km alt
D at 306km alt
Northward Efield (mVm⁻¹)
at 278km alt
ABC at 250km alt
BCD at 250km alt
Eastward Efield (mVm⁻¹)
CDA at 250km alt
DAB at 250km alt
at 278km alt
UT
UT

[1988]. Next, we will discuss what defines the duration of the DUSE referring the observation of background parameter obtained by the EISCAT.

3.2. EISCAT Observations

[15] During the interval of event A, CP-1 mode was running in the EISCAT mainland system, and during the interval of event B, CP-2 mode was running. Here, we introduce the data obtained by the EISCAT UHF system during both events. The observations are summarized in Figure 4 together with the latitude-time-parameter plots of the CUTLASS Finland line-of-sight velocity for comparison.

3.2.1. Event A: 14 February 1996

[16] The left top panel show the line-of-sight Doppler velocity observed by the CUTLASS Finland radar beam 5 from 0800 UT to 1600 UT on 14 February 1996, which is plotted as a function of geographic latitude and universal time. As mentioned before, for EISCAT CP-1 mode, the F region intersection volume lies within range gate 16 of beam 5 of the Finland radar field of view, which is indicated by the horizontal dashed line. The two vertical lines indicate the duration of the DUSE from 1230 UT to 1425 UT. It is clearly seen that the EISCAT CP-1 beam is located within the DUSE and thus is able to provide information on the background ionospheric parameters during the DUSE observed on this day.

[17] The observations of EISCAT CP-1 mode are summarized in the left middle four panels of Figure 4, where altitude versus UT plots of electron density, ion and electron temperature for the altitude range from 150 to 500 km and electron density at F region altitude (300 km) are shown. In the panel of electron density at 300 km altitude, variation of electron density derived from IRI90 model [*Bilitza*, 1990] is overplotted as a background shadow. Before the onset of the DUSE, the electron density seems to be controlled by the solar illumination. Soon after the onset of the DUSE, the electron density starts to decrease and some 30 min after the disappearance of the DUSE the electron density stops decreasing, which is most clearly seen in the panel of electron density at 300 km altitude. The level of the electron density reduction is apparently larger than that estimated by the IRI90 model. This signature suggests that the field of view of the EISCAT CP-1 beam crosses the Sunward edge of the trough during the interval of the DUSE. The other signature worth noting is that an increase of ion temperature can be found during the interval between 1330 UT and 1520 UT. Previous studies of morphological feature of the trough [e.g., *Rodger et al.*, 1992] indicated that plasma temperature is normally high within the midlatitude trough. Hence this increase of ion temperature observed by the EISCAT suggests that the field of view of the EISCAT CP-1 enters the midlatitude trough through its duskside edge. In general, the midlatitude trough moves equatorward with increasing MLT [*Collis and Haggstrom*, 1988; *Rodger et al.*, 1992]; hence the beam of EISCAT CP-1 mode is considered to move out of trough and enter into the auroral oval after 1520 UT when the enhancement of ion temperature ends.

[18] The left bottom two panels display the geographic northward and eastward components of the electric field obtained from the tristatic velocity determination at 278 km altitude. Following the appearance of the DUSE, the northward electric field starts to increase from $\approx$20 mV m^{-1} to $\approx$50 mV m^{-1}, while there is little variation in the eastward component. *Collis and Haggstrom* [1988] and *Haggstrom and Collis* [1990] demonstrated an observation of Sunward extension of the midlatitude trough with a rapid westward plasma drift and an enhancement of ion temperature. This situation has been reproduced numerically by *Namgaladze et al.* [1996] and was considered to be rather typical for substorm conditions. They concluded that the Sunward movement of the duskside edge of the trough is caused by the increase of the loss rate through the ion-frictional heating due to the enhanced relative velocity between the ion and neutral populations (for the detail of the ion-frictional heating, see *Rees and Walker* [1968], *Schunk* [1975], and *Schunk and Sojka* [1982]). In our observation, the parameters observed by the EISCAT radar exhibit a very similar behavior to those reported by *Collis and Haggstrom* [1988] and *Haggstrom and Collis* [1990]. On the basis of this similarity, the increase of the ion temperature and the reduction of the electron density in our observation seem to be a manifestation of the ion-frictional heating due to the strong northward electric field. These strong electric field signatures in the subauroral F region ionosphere could be originated from the occurrence of the substorm and might correspond to the feature known as the subauroral ion drift (SAID) [*Galperin et al.*, 1973; *Smiddy et al.*, 1977; *Anderson et al.*, 1991, 1993, 2001; *Karlsson et al.*, 1998]. Detailed discussion on generation mechanism of the trough responsible for the DUSE during this interval and its association with the strong northward electric field will be given in section 4.

3.2.2. Event B: 12 October 1996

[19] The top right panel of Figure 4 show the line-of-sight Doppler velocity observed by the CUTLASS Finland radar beam 5 from 0800 UT to 1600 UT on 12 October 1996. The

Figure 4. (opposite) Summary of the observations by the EISCAT UHF system for the two intervals of interest. The top two panels show the line-of-sight Doppler velocity observed by the CUTLASS Finland radar beam 5 from 0800 UT to 1600 UT on 14 February 1996 (left)and on 12 October 1996 (right). Horizontal dashed line indicates the latitude of gate 16 of Finland radar beam 5 which is a common volume with the EISCAT UHF system. Two vertical lines indicate duration of the DUSE for both events. Observations of the EISCATUHF system during both events are displayed in middle eight panels for event A (left) and for event B (right), where altitude profile of the electron density, ion temperature, electron temperature up to 500 km altitude, and electron density at 300 km altitude are shown. In the panel of electron density at 300 km altitude, electron density variation derived from IRI90 model is overplotted as a shadow. In the case of event B, observations of all four beams of the EISCAT CP-2 mode are plotted together. The bottom four panels indicate the geographic northward and eastward components of the electric field obtained from tristatic observation at 278 km altitude for event A (left) and determined from beam-swinging technique at 250 km altitude for event B(right). See color version of this figure at back of this issue.

format is same as before. For the field-aligned pointing beam of EISCAT CP-2 mode, the F region intersection volume also lies within range gate 16 of beam 5 of the Finland radar field of view and the horizontal dashed line indicates the latitude of gate 16 of Finland radar beam 5. Two vertical lines indicate the duration of the DUSE, which is 65 min from 1310 UT to 1415 UT. The fields of view of the EISCAT CP-2 beams are located within the region of the DUSE, and hence it is again possible to compare the observation of the Finland radar and the EISCAT CP-2 mode directly.

[20] The right middle four panels indicate the observation of EISCAT CP-2 mode during this interval, where altitude profiles of the electron density, ion temperature, electron temperature for altitude range from 150 to 500 km, and electron density at F region altitude are shown. Here, data from all beams of the CP-2 mode are plotted together. Electron density variation predicted by the IRI90 model is also displayed as a shadow in the panel of the electron density at 300 km altitude. During the period of the DUSE appearance, the EISCAT observed a rapid decrease of electron density. Also, a clear increase of ion temperature was identified after the disappearance of the DUSE. These signatures suggest that the EISCAT CP-2 beams start to encounter the Sunward edge of the trough at the time of the DUSE onset, and after the DUSE disappears the EISCAT CP-2 beams are located completely within the trough. What is worth noting is that the duration of the electron density decrease is quite similar to the duration of the DUSE, which means that the duration time of the DUSE is defined by the scale of the electron density decrease.

[21] The bottom right two panels display the geographic northward and eastward components of the electric field determined by a beam-swinging technique using the data of three beams out of four CP-2 beams at 250 km altitude. During this interval the data of the remote sites (Kiruna and Sodankyla) contain large error, then the tristatic velocity measurement could not be applied for the determination of two-dimensional electric field. Following the appearance of the DUSE, the northward electric field starts to increase from $\approx$10 mV m^{-1} to 45 mV m^{-1}, while there is no considerable variation in the eastward component. The parameters observed during this event exhibit a behavior quite similar to those during event A, which indicates that the background conditions of the DUSE presented here is a reproducible feature in the EISCAT observations during disturbed conditions within these local times. Again the large values of the electric field imply that the trough observed during this interval could be associated with the rapid convection in the subauroral ionosphere during substorm. A relationship of this strong northward electric field with the occurrence of the substorm will be discussed employing data of ground magnetic field variation on the nightside in the later part of this section.

3.2.3. Background Parameters in the Absence of the DUSE

[22] We have examined a behavior of background parameters of the DUSE and have confirmed the model proposed by *Hosokawa et al.* [2001]. In short, steep electron density gradient in a longitudinal direction, which is considered to correspond to the Sunward edge of the trough, has been observed in the vicinity of the DUSE. However, we have demonstrated no evidence that the electron density gradient identified by the EISCAT radar is absolutely responsible for the generation of the DUSE in this region. Hence we need to show how background parameters behave when the DUSE does not appear. Figure 5 displays observations from the

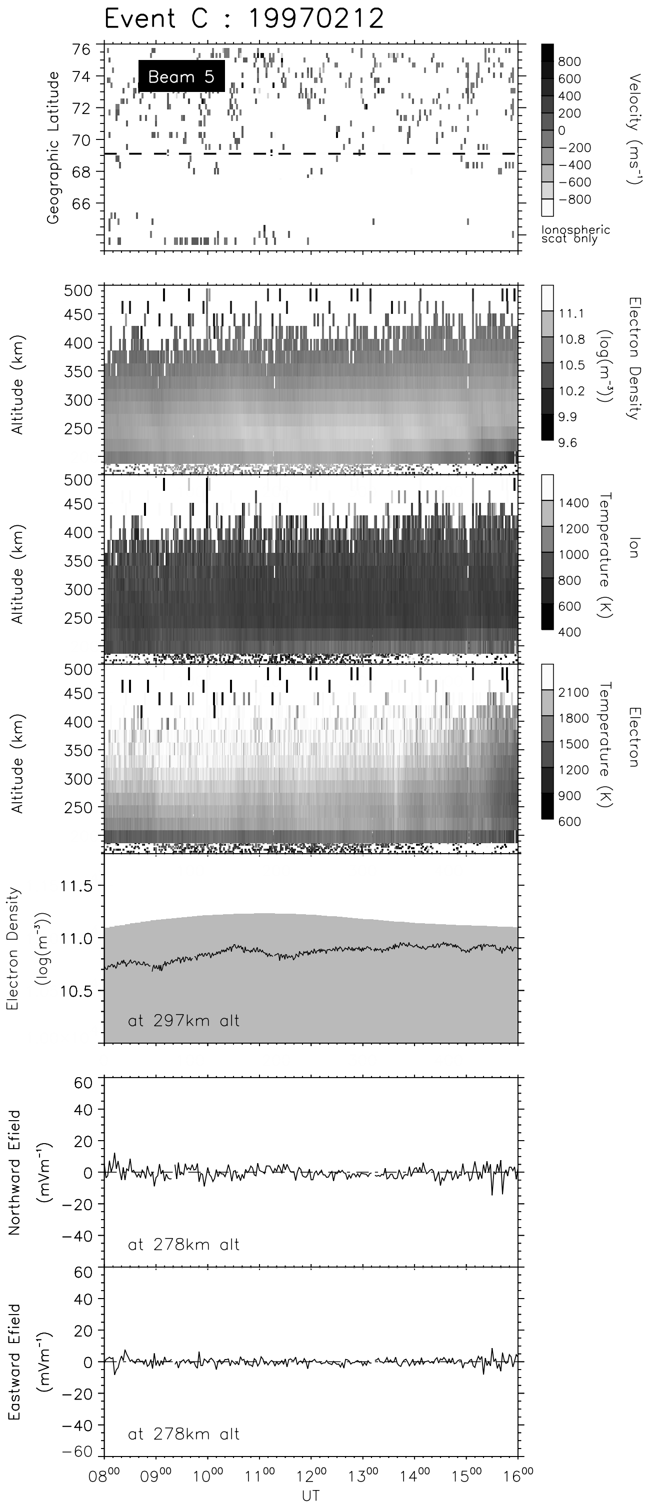

Figure 5. Summary of the observations from the CUTLASS Finland and the EISCAT UHF system for event C (12 February 1997), in which the DUSE was not observed by the CUTLASS Finland radar. See color version of this figure at back of this issue.

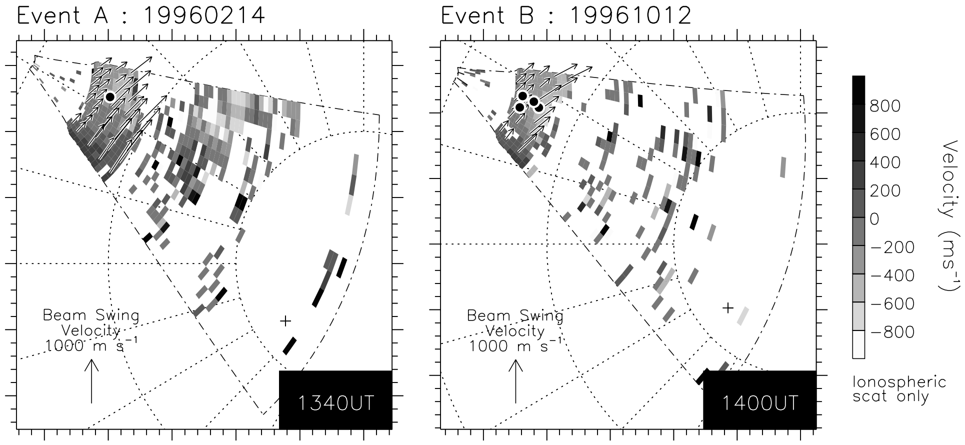

Figure 6. Line-of-sight Doppler velocity measurements from the CUTLASS Finland radar for selected scans of both intervals(1340 UT for event A and 1400 UT for event B, respectively),superimposed on which are two-dimensional velocity vectors estimated by applying a beam-swinging technique on the line-of-sight Doppler velocities. See color version of this figure at back of this issue.

CUTLASS Finland and the EISCAT UHF system on 12 February 1997 (hereinafter referred as event C). On this day the DUSE did not appear in the field of view of the CUTLASS Finland radar (see top panel in Figure 5). Background parameters observed by the EISCAT UHF system CP-1 mode are displayed in the bottom six panels of Figure 5 in the same format as Figure 4, which show that there exists no specific variation in electron density, ion temperature, and electric field observations. This observation strongly suggests that the steep Sunward directed plasma density gradient and the strong northward electric field observed in the vicinity of the DUSE during events A and B play an indispensable role for the generation of the DUSE.

3.3. Plasma Drift Observation by the CUTLASS Finland Radar

[23] During the intervals of events A and B the EISCAT radar observes large northward directed electric field up to 50 mV m^{-1} in the vicinity of the DUSE. Here, we compare the velocity measurement from the CUTLASS Finland radar with the electric field observation from the EISCAT radar. Purpose of this comparison is to confirm a consistency of the simultaneous observation from the radars of different scattering techniques. Figure 6 displays the line-of-sight velocity measurement from the CUTLASS Finland radar for selected scans of both intervals (1340 UT for event A and 1400 UT for event B, respectively), superimposed on which are two-dimensional velocity vectors estimated by a beam-swinging technique [see *Ruohoniemi et al.*, 1989; *Freeman et al.*, 1991; *Milan et al.*, 2000]. When a beam-swinging technique is applied, it is assumed that the flow within each backscatter region is uniform across the field of view; in other words, the zonal and meridional components relative to the local L shell are constant at all points. Within the region of interest in this paper, convective flow is expected to be zonal (westward); then the estimated two-dimensional velocity is considered to be reliable. In the same manner as Figure 3, the closed circles indicate the field of view of the EISCAT beams at F region altitudes. There were comprehensive comparisons of the velocities obtained from the CUTLASS Finland radar and from the EISCAT radar [*Davies et al.*, 1999, 2000]. The authors concluded that there is an overall reasonable correspondence between these two measurements. At the time of the scans presented in Figure 6, two-dimensional velocity determined from the line-of-sight Doppler velocity of the Finland radar is $\sim$600 m s^{-1} westward (corresponding-electric field is $\sim$30 mV m^{-1} northward) within the field of view of the EISCAT beams, which is in good agreement with the electric field measurement by the EISCAT UHF system presented in Figure 4. This good agreement supports a validity of our simultaneous measurement of the DUSE using the two different observation techniques.

3.4. Ground Magnetometer Observations

[24] During both intervals of this study the EISCAT observed an enhanced subauroral electric field in the vicinity of the DUSE and corresponding trough structure. In general, these high-speed plasma drifts in the duskside subauroral region are connected with the occurrence of the geomagnetic substorm on the nightside ionosphere. One famous signature of these high-speed plasma flows associated with the substorm is a feature known as the subauroral ion drift (SAID). We cannot determine whether the strong northward electric field observed during the intervals of this study is the SAID or not. However, there still exists a possibility that this large electric field results from the substorm activity. Here, we check the occurrence of the substorm using the data of magnetometer stations from the Canadian Auroral Network for the OPEN Program Unified Study (CANOPUS) network (as described by *Samson et al.*, 1992) and discuss a relationship between the electric field enhancement and substorm activity. Figure 7 shows X-component magnetograms and bandpass filtered data of the DAWS station (magnetic latitude is 65.93°) conveniently located on the nightside for the three intervals of interest.

[25] In the case of event A (top panel), a substorm occurs at 1120 UT (DAWS is located at 0035 MLT), which is 70 min before the onset of the DUSE. The occurrence of the substorm is confirmed by large negative bay in the X-component and the presence of Pi2 pulsations indicating the expansion phase onset of the substorm. In the case of event

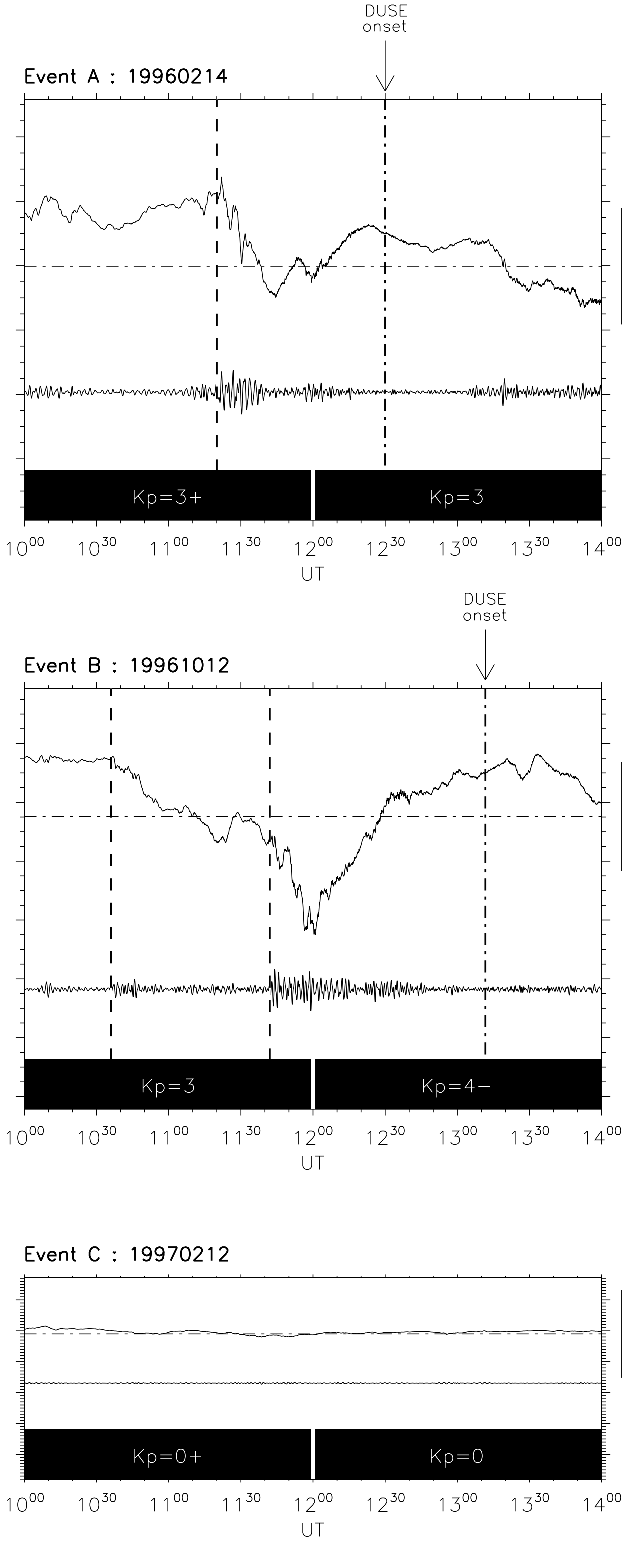

Figure 7. X-component magnetograms from the DAWS station of the CANOPUS networks, along with filtered data showing Pi2 activity (scaled by a factor of 5 for clarity) for the three intervals of interest in this paper. Vertical dashed lines indicate the onset of the substorm breakup and vertical dash-dotted lines the onset of the DUSE.

B (middle panel), two substorm signatures are identified. The first substorm occurs at 1035 UT and the second at 1312 UT (DAWS is located at 2351 MLT and 0058 MLT, respectively). The negative bay in the X-component is deeper in event B than that in event A. This means that the level of the geomagnetic disturbance is more severe in event B than that in event A, which is consistent with *Kp* indices. The bottom panel shows the observation of the DAWS station during event C in which the DUSE was not observed by the CUTLASS Finland radar. In contrast to the observations during events A and B, there can be found no clear signature of the substorm breakup, which is consistent with the lack of the large northward electric field in the duskside subauroral region and the absence of the DUSE in the field of view of the CUTLASS Finland radar.

4. Discussions

4.1. Model

[26] In order to confirm the generation mechanism of the DUSE proposed by *Hosokawa et al.* [2001], we have investigated two examples of the DUSE which had been commonly observed by the CUTLASS Finland radar and the EISCAT UHF system. As a result, when the DUSE appeared in the field of view of the CUTLASS Finland radar, the EISCAT observed a Sunward directed density gradient in the vicinity of the DUSE. This density gradient was rather steeper than those created only by the solar illumination around sunset. Also, after the passage of the DUSE, EISCAT observed an enhancement in ion temperature, which suggested that the EISCAT entered the midlatitude trough through the edge of the midlatitude trough (to be exact we cannot identify whether this edge corresponds duskside or equatorward edge only from the present observations). In addition, a strong northward electric field, which is identical to westward plasma drift, was identified during the intervals of interest. These observations show that the geometry of the background parameters around the DUSE is quite consistent with the situation predicted by *Hosokawa et al.* [2001] and strongly support the validity of their model.

[27] Here, we discuss the generation of the DUSE by estimating the growth rate of FAIs quantitatively. Ionospheric FAIs are density fluctuations which have been amplified in plasma instability processes [*Fejer and Kelley*, 1980; *Keskinen and Ossakow*, 1983; *Tsunoda*, 1988]. The model proposed by *Hosokawa et al.* [2001] is based on the gradient drift instability process, in which the linear growth rate of the density fluctuation γ is proportional to the plasma velocity V_0 and inversely proportional to the scale length of the background plasma density gradient, L, i.e., $\gamma \propto V_0/L$, where $V_0 = E_0/B$, $L = n_0/\nabla n_0$. B is the magnitude of the geomagnetic field, E_0 is the magnitude of the electric field in the plane perpendicular to $\mathbf{B}$, and n_0 is the background plasma density. In practice, the growth of FAIs competes with plasma diffusion; hence the complete growth rate of FAIs by the gradient drift instability is

$$\gamma_c \propto \frac{V_0}{L} - k^2 D = \frac{E_0}{B} \cdot \frac{\nabla n_0}{n_0} - k^2 D,$$

where k is the wave number of FAIs, and D is the diffusion coefficient. This equation means that if the complete growth rate γ_c is greater than zero, FAIs whose wave number is equal to k ($\lambda = 2\pi/k$ is equivalent to the scale of the FAIs) can grow by overcoming the diffusion effect. Assuming γ_c is zero, we can obtain the maximum wave number, k_{max} and associated minimum wavelength, λ_{min}, of the FAIs which can survive in this region. Backscatter of radar radio wave, $\mathbf{k_r}$, occurs from FAIs with wave vector, $\mathbf{k}$, which satisfy the condition $\mathbf{k} = \pm 2\mathbf{k_r}$. During both intervals, the operating frequency of the CUTLASS Finland radar was approximately 9.98 MHz; hence the wavelength ($\lambda = 2\pi/2k_r$) of the FAIs which could be observed by the radar was $\sim$15 m. If the calculated minimum wavelength, λ_{min}, is shorter than 15 m, the SuperDARN radars can observe FAIs generated directly by the gradient drift instability.

[28] *Hosokawa et al.* [2001] calculated the growth rate of FAIs responsible for the DUSE using values from several models and suggested that a cascade process of FAIs from larger scale to smaller scale is needed for the generation of the DUSE. However, they could not carry out a growth rate calculation of the DUSE using observed background parameters. Here, we employ the background parameters observed by EISCAT and clarify whether the cascade process is still required or not. For comparison we use the same diffusion coefficient as that used in *Hosokawa et al.* [2001],

$$D = \frac{2k_B T_e \nu_{ei} m_e}{e^2 B^2},$$

where k_B is the Boltzmann constant, and e, T_e, and m_e are the electron charge, temperature, and mass, respectively. Now we discuss the F region FAIs, so the collision frequency between electrons and ions is considered [*Kelley*, 1989],

$$\nu_{ei} = \left[34 + 4.18 \ln\left(T_e^3/n_e\right)\right] n_e T_e^{-3/2}.$$

For both events the geomagnetic field is set to 4.56×10^4 nT (from the International Geomagnetic Reference Field 2000 model) as a value over Tromsoe. When we calculate ∇n_e, it is assume that the electron density variation observed by the EISCAT is predominantly spatial. In the case of the event A, calculation is carried out using observations at 1330 UT, at which $n_e = 9.37 \times 10^{10}$ m^{-3}, $\nabla n_e = 1.01 \times 10^5$ m^{-4} (variation in n_e between 1310 UT and 1350 UT is divided by the length of the movement of the EISCAT), $T_e = 2006$ K, and $E = 38.5$ mV m^{-1}, giving a maximum wave number $k_{max} = 0.151$ m^{-1} and minimum wavelength $\lambda_{min} = 41.54$ m. In the case of the event B, observations at 1350 UT are used for the growth rate calculation, at which $n_e = 9.59 \times 10^{10}$ m^{-3}, $\nabla n_e = 1.53 \times 10^5$ m^{-4} (variation in n_e between 1330 UT and 1410 UT is employed), $T_e = 1546$ K, and $E = 24.5$ mV m^{-1}, giving a maximum wave number $k_{max} = 0.137$ m^{-1} and minimum wavelength $\lambda_{min} = 45.72$ m. During both intervals the calculated minimum wavelength is still larger than the scale of FAIs which can be observed by the Finland radar. This result suggests that a cascade process from larger-scale FAIs to smaller scale is also working during these events and, most likely, is always needed to explain the generation of the DUSE.

4.2. Generation Mechanisms of the Trough

[29] Both *Ruohoniemi et al.* [1988] and *Hosokawa et al.* [2001] pointed out that the source of the DUSE lies at magnetic latitudes associated with the midlatitude trough. Previous studies proposed that the primary cause of the formation of the trough during quiet geomagnetic condition is a loss through recombination in darkened regions of stagnated plasma (stagnation trough theory) [*Knudsen*, 1974; *Knudsen et al.*, 1977; *Spiro et al.*, 1978]. Competition between the Earth corotation and ionospheric convection forms a region of stagnated plasma in the evening sector. Flux tubes of F region plasma have long trajectories in darkness before being transported into sunlit, and then the trough is formed by a loss through ordinary recombination in darkness. If we do not consider an advection of the low-density plasma by the subauroral convection into the sunlit hemisphere, the Sunward edge of the trough is expected to be located at the evening side of the local sunset (i.e., the trough is formed in the dark hemisphere). Since the DUSE normally appears when the solar zenith angle is near 95°, the DUSE during quiet condition can be explained by the stagnation trough theory.

[30] On the other hand, the present observation demonstrated that local time where the DUSE appears extended into the dayside further across the terminator during disturbed conditions. Also, the Sunward edge of the trough, where a steep Sunward electron density gradient exists, was shifted to the earlier local time sector together with the DUSE. These features are in good agreement with the results of the statistical analysis of the DUSE by *Hosokawa et al.* [2001]. In addition, the EISCAT UHF system observed elevated ion temperature and strong poleward electric field (up to 50 mV m^{-1}) in the vicinity the DUSE and the reduction of electron density. Then the question addressed here is how the Sunward edge of the trough responsible for the DUSE is formed at the earlier local time sector in our observations. There are at least two possible mechanisms which could contribute to this Sunward extension of the DUSE and trough.

[31] One of them employs an enhanced advection of low density plasma from the stagnation region in darkness into the sunlit hemisphere by substorm-induced subauroral convection. As geomagnetic activity increases, northward electric field in the subauroral region, which corresponds to the westward convective return flow in the dusk sector, also increases. Therefore plasma that has been stagnated in darkness can be transported further across the terminator before it becomes filled in with local solar production. *Sojka et al.* [1983] simulated the dayside extension of the trough numerically and suggested that this extension can be due to transport of low-density nightside flux tubes to the sunlit region across the terminator. In practice, it is difficult to estimate to what degree this effect contribute to the Sunward extension of the trough only from the present observations. However, observed westward flow (1 km s^{-1} at maximum) is comparable to that used in the calculation by *Sojka et al.* [1983], which suggests that the effect of the substorm-related enhanced advection should not be ignored in our observation.

[32] The other employs an enhanced recombination trough theory [*Evans et al.*, 1983; *Holt et al.*, 1983; *Providakes et al.*, 1989]. These authors have reported that the trough is formed by an enhanced recombination in regions of rapid subauroral plasma drift associated with substorm activity through ion-frictional heating. *Schunk et al.* [1975] have numerically

estimated the effect of electric field on the electron density depletion in the F region through an interaction between ions and neutrals. They have pointed out that electric field in a rest frame of neutrals $\approx$50 mV m^{-1} substantially reduces electron density in the F region altitudes. For the case of event A, electric field observation was terminated before EISCAT entered the trough. Hence we cannot know whether the electric field within the trough is sufficient for the frictional heating. However, electric field observation in event B shows that there exist occasions when the northward electric field exceeds 50 mV m^{-1} (between 1440 and 1510 UT). During this period elevated ion temperature up to 1500 K is also observed at 300 km altitudes. Although we do not have exact information on the neutral wind velocity on that occasion, combination of the strong northward electric field and elevated ion temperature suggests a possibility that the density depletion within the trough during our observations is connected to an enhancement of recombination caused by the ion-frictional heating. *Davies et al.* [1997] have performed a statistical investigation of the occurrence of the ion-frictional heating observed by the EISCAT UHF system. They demonstrated that the ion-frictional heating occurs predominantly in the dusk sector rather than the dawn sector and the region where the heating is observed by the EISCAT gradually moves to the earlier local time sector with the *Kp* index increasing. This statistical result also supports our suggestion that the dayside displacement of the DUSE can be caused by the Sunward extension of the trough due to the loss through the ion-frictional heating process associated with the fast ion drift within the trough.

4.3. Relationship With the Other Phenomena

[33] We cannot decide which of the above mechanisms primally contributes to the Sunward extension of the trough in our observation. However, both of the hypotheses commonly assume the existence of the enhanced electric field, which implies that the enhanced electric field is the key to explain the Sunward extension of the trough and DUSE. Here we discuss the origin of this large electric field. There have been a number of observations of the rapid convective flows in the duskside subauroral region [e.g., *Anderson et al.*, 1991, 1993; *Freeman et al.*, 1992; *Shand et al.*, 1998]. Since these rapid plasma drift signatures, referred to as subauroral ion drift (SAID) or substorm associated radar auroral surge (SARAS), were suggested to occur well after the substorm onset (most clearly seen in statistical analysis of the SAID by *Karlsson et al.* [1998]). Then, the SAID/SARAS were interpreted as indicating an ionospheric response that would be established in the magnetosphere after development of the substorm expansion [*Freeman et al.*, 1992; *Anderson et al.*, 1993, 2001]. The definition of SAID given by *Spiro et al.* [1979, p. 659] is "the portion of the Sunward flow equatorward of the auroral zone that exceeds 500 m s^{-1}," that of *Anderson et al.* [1991, p. 5786] is "westward plasma flow exceeding 1000 m s^{-1}," and that of *Karlsson et al.* [1998, p. 4328] is "poleward electric field exceeding 30 mV m^{-1} ($\approx$600 m s^{-1} in these latitudes)." Owing to the lack of the observation in the other area of the subauroral ionosphere, especially premidnight sector, we can not provide a clear evidence that the high-speed westward flow reported in this paper belongs to the category classified as SAID/SARAS. However, there exist occasions when the northward electric field exceeds 50 mV m^{-1} ($\approx$1 km s^{-1} westward drift) and the occurrence of the substorm is evidenced by a large negative bay and the presence of Pi2 pulsations in the CANOPUS magnetometers on the nightside before the onset of the DUSE. These observational facts suggest a possibility that the strong electric field could be classified as the category of SAID/SARAS.

[34] Now we turn to discuss how the morphological feature of the DUSE (degree of the Sunward extension, etc.) can be utilized as a tool for estimating condition of magnetosphere-ionosphere coupling system around the subauroral latitudes. Discussion in this part is on the assumption that the enhanced electric field due to the SAID/SARAS type phenomenon forms the trough responsible for the DUSE through the frictional-heating process. As noted in the previous section, the degree of the sunward extension of the region where the DUSE appears is larger in event B than that in event A. Furthermore, the magnitude of the geomagnetic field variation associated with the substorm breakup is found to be larger in event B than that in event A. Although we just examine the difference between these two DUSE events, however, this implies that degree of the Sunward movement of the DUSE tells us how far the high-speed convective flow associated with the SAID/SARAS penetrates into the earlier local time sector. *Southwood and Wolf* [1978] suggested that SAID is generated as a result of the establishment of low-latitude shielding of substorm-enhanced electric fields. An increase in the cross-tail magnetospheric electric field induces an electric field between the inner edges of the electron and proton ring currents when their separation is small. Recently, *De Keyser et al.* [1998] and *De Keyser* [1999] pointed out that the SAID is ionospheric footprint of a localized intense electric field generated on a current sheet that separates the cold magnetospheric plasma from the energetic particles penetrating into the inner magnetosphere during the substorm. If we assume that the strong northward electric field detected in the present observations belongs to the SAID/SARAS, the idea proposed by De Keyser and colleagues allows us to expect that the location where the DUSE appears can be used as a diagnostic tool to estimate how far the energetic particles does penetrate into the inner magnetosphere from the plasma sheet during substorm. There have been direct observations of this particle penetration close to 1800 MLT in the magnetosphere [e.g., *Ejiri et al.*, 1980]. In order to know whether this hypothesis is true or false, a relationship between an enhancement of the subauroral electric field and particle penetration into the inner magnetosphere must be investigated in relation to the appearance of the DUSE.

[35] Stable auroral red (SAR) arcs are one of the other outstanding phenomena in the subauroral ionosphere. Relationship between SAR arc and trough has been clearly shown by *Mendillo et al.* [1987]. *Foster et al.* [1994] have demonstrated that SAR arc is colocated with trough and a region of enhanced westward convection of similar width. They indicated that the convection feature seen in association with the SAR arc had many of the characteristics of the SAID event. These observational facts suggest that the SAR arcs are also caused by the ion-frictional heating process due to the strong electric field (possibly SAID). If we examine optical observation during the interval of this

study, the DUSE might appear at the Sunward edge of the visible SAR arc. Recently, M. L. Parkinson et al. (On the lifetime and extent of an auroral westward flow channel (AWFC) observed during a magnetospheric substorm, submitted to Annales Geophysicae, 2002) have presented a signature of strong Sunward flow channel (maximum velocity is $\sim$1.3 km s^{-1}) at subauroral latitudes well after the substorm expansion phase onset. They concluded that this flow satisfies all of the criteria defining the SAID.To acquire more conclusive results, coordinated observation of the subauroral phenomena such as DUSE, SAID/SARAS, and SAR arcs using various instruments involving all of the SuperDARN chain is needed in the near future.

5. Summary and Conclusions

[36] Dusk scatter event (DUSE) (first reported by *Ruohoniemi et al.* [1988]) is a most reproducible feature of the SuperDARN radar backscatter within the subauroral F region ionosphere. *Hosokawa et al.* [2001] pointed out that the region where the DUSE appears has a close relationship with the duskside end of the midlatitude trough in longitudinal direction and proposed a model explaining the generation of the DUSE which employs a Sunward density gradient at the duskside edge of the trough together with an ambient poleward electric field. In order to exhibit the evidence that the model proposed by *Hosokawa et al.* [2001] is correct, we have investigated two DUSE events(referred as events A and B in the text) which had been observed by the CUTLASS Finland radar and the EISCAT UHF system simultaneously. Consequently, when the DUSE is observed by the Finland radar, the EISCAT observed Sunward directed density gradient in the vicinity of the DUSE. This density gradient was steeper than those expected to exist around sunset under the control of solar illumination. Also, after the passage of the DUSE, the EISCAT observed ion temperature enhancement, which means that the EISCAT entered the midlatitude trough through its duskside edge. These observations show that geometry of the parameters around the DUSE is quite consistent with the model proposed by *Hosokawa et al.* [2001] and strongly suggest the validity of their model.

[37] In addition, the EISCAT observed an enhancement of the poleward electric field around the DUSE, and a signature of the substorm breakup was identified by the ground magnetometer on the nightside. On the basis of these observations, we suggest that the dayside extension of the midlatitude trough responsible for the generation of the DUSE during the intervals of interest was primarily formed and maintained by an enhanced recombination in the region of rapid convective flows associated with the substorm activity through the ion-frictional heating process, although an enhanced advection of low-density plasma across the terminator also made an additional contribution. We employed substantial background parameters observed by the EISCAT and calculated linear growth rate of the DUSE. During both intervals the calculated minimum wavelength of FAIs is still larger than the scale of FAIs observed by the Finland radar. This result suggests that cascade process from larger-scale FAIs to smaller scale is also working during these events and is still needed to explain the generation of the DUSE. During both intervals of this study, substorm occurs on the nightside and local time where the DUSE appears extends into the dayside. Degree of the extension is larger in event B than that in event A, and the level of the geomagnetic disturbance is found to be more severe in event B than that in event A. This means that degree of extension of the DUSE into the dayside could be used to estimate the level of the disturbance associated with the substorm in the subauroral F region ionosphere.

[38] **Acknowledgments.** The Iceland East-Finland radar pair (the Cooperative UK Twin Located Auroral Sounding System: CUTLASS) is funded by the Particle Physics and Astronomy Research Council, U.K., under grantPPA/R/R/1997/00256, the Finnish Meteorological Institute, Helsinki, and the Swedish Institute for Space Research, Uppsala. We are indebted to the Director and staff of EISCAT for operating the facility and supplying the data. EISCAT is an International Association supported by Finland (SA), France (CNRS), the Federal Republic of Germany (MPG), Japan (NIPR), Norway (NFR), Sweden(NFR) and the United Kingdom (PPARC). CANOPUS instrument array, constructed, maintained, and operated by the Canadian Space Agency, provided the data used in this study. This research is supported by the Grant-in Aid for Scientific Research(A:11304029) from Japan Society for the Promotion of Science(JSPS). One of the authors (K.H.) is supported by a grant of Research Fellowships of the Japan Society for the Promotion of Science (JSPS) for Young Scientists.

[39] Arthur Richmond thanks Johan De Keyser and Alan S. Rodger for their assistance in evaluating this paper.

References

Anderson, P. C., W. B. Hanson, and R. A. Heelis, The ionospheric signatures of rapid subauroral ion drifts, *J. Geophys. Res.*, *96*, 5792, 1991.

Anderson, P. C., W. B. Hanson, R. A. Heelis, J. D. Craven, D. N. Baker, and L. A. Frank, A proposed production model of rapid subauroral ion drifts and their relationship to substorm evolution, *J. Geophys. Res.*, *98*, 6069, 1993.

Anderson, P. C., D. L. Carpenter, K. Tsuruda, T. Mukai, and F. J. Rich, Multisatellite observations of rapid subauroral ion drifts (SAID), *J. Geophys. Res.*, *106*, 29,585, 2001.

Baker, K. B., and S. Wing, A new magnetic coordinate system for conjugate studies of high latitudes, *J. Geophys. Res.*, *94*, 9139, 1989.

Bilitza, D., International Reference Ionosphere 1990, *NSSDC/WDC-A-R & S 90-22*, Nat. Space Sci. Data Cent.,World Data Cent. A for Rocket and Satell., Greenbelt, Md., 1990.

Collis, P. N., and I. Haggstrom, Plasma convection and auroral precipitation processes associated with the main ionospheric trough at high latitudes, *J. Atmos. Terr. Phys.*, *50*, 389, 1988.

Davies, J. A., M. Lester, and I. W. McCrea, A statistical study of ion frictional heating observed by EISCAT, *Ann. Geophys.*, *15*, 1399, 1997.

Davies, J. A., M. Lester, S. E. Milan, and T. K. Yeoman, A comparison of velocity measurements from the CUTLASS Finland radar and the EISCAT UHF system, *Ann. Geophys.*, *17*, 892, 1999.

Davies, J. A., T. K. Yeoman, M. Lester, and S. E. Milan, A comparison of F-region ion velocity observations from the EISCAT Svalbard and VHF radars with irregularity drift velocity measurement from the CUTLASS Finland HF radar, *Ann. Geophys.*, *18*, 589, 2000.

De Keyser, J., Formation and evolution of subauroral ion drifts in the course of a substorm, *J. Geophys. Res.*, *104*, 12,339, 1999.

De Keyser, J., M. Roth, and J. Lemaire, The magnetospheric driver of subauroral ion drifts, *Geophys. Res. Lett.*, *25*, 1625, 1998.

Ejiri, M., R. A. Hoffman, and P. H. Smith, Energetic particle penetrations into the inner magnetosphere, *J. Geophys. Res.*, *85*, 653, 1980.

Evans, J. V., J. M. Holt, W. L. Oliver, and R. H. Wand, The fossil theory of nighttime high latitude F region troughs, *J.Geophys. Res.*, *88*, 7769, 1983.

Fejer, B. G., and M. C. Kelley, Ionospheric irregularities, *Rev. Geophys*, *18*, 401, 1980.

Feldstein, Y. I., and G. V. Starkov, Dynamics of auroral belt and polar geomagnetic disturbance, *Planet. Space Sci.*, *15*, 209, 1967.

Foster, J. C., M. J. Buonsanto, M. Mendillo, D. Nottingham, F. J. Rich, and W. Denig, Coordinated stable auroral red arcobservations: Relationship to plasma convection, *J. Geophys. Res.*, *99*, 11,429, 1994.

Freeman, M. P., J. M. Ruohoniemi, and R. A. Greenwald, The determination of time-stationary two-dimensional convection patterns with single-station radars, *J. Geophys. Res.*, *96*, 15,735, 1991.

Freeman, M. P., D. J. Southwood, M. Lester, T. K. Yeoman, and G. D. Reeves, Substorm-associated radar auroral surges, *J. Geophys. Res.*, *97*, 12,173, 1992.

Galperin, Y. I., V. N. Ponomarev, and A. G. Zosimove, Direct measurements of ion drift velocity in the upper atmosphere during a magnetic storm, *Kosm. Issled.*, *11*, 273, 1973.

Greenwald, R. A., et al., DARN/SuperDARN: A global view of high-latitude convection, *Space Sci. Rev.*, *71*, 763, 1995.

Haggstrom, I., and P. N. Collis, Ion composition changes during F-region troughs, *J. Atmos. Terr. Phys.*, *52*, 519, 1990.

Halcrow, B. W., and J. S. Nisbet, A model of F2 peak electron density in the main trough regionof the ionosphere, *Radio Sci.*, *5*, 815, 1977.

Holt, J. M., J. V. Evans, and R. H. Wand, Millstone Hill studies of the trough: Boundary between the plasmapause and magnetosphere or not?, *Radio Sci.*, *18*, 947, 1983.

Holzworth, R. H., and C. I. Meng, Mathematical representation of the auroral oval, *Geophys. Res. Lett.*, *2*, 377, 1975.

Hosokawa, K., T. Iyemori, A. S. Yukimatu, and N. Sato, Source of field-aligned irregularities in the subauroral F region as observed by the SuperDARN radars, *J. Geophys. Res.*, *106*, 24,713, 2001.

Karlsson, T., G. T. Marklund, L. G. Blomberg, and A. Mälkki, Subauroral electric fields observed by the Freja satellite: A statistical study, *J. Geophys. Res.*, *103*, 4327, 1998.

Kelley, M. C., *The Earth's Ionosphere*, Academic, San Diego,Calif., 1989.

Keskinen, M. J., and S. L. Ossakow, Theories of high-latitude ionospheric irregularities: A review, *Radio Sci.*, *18*, 1077, 1983.

Knudsen, W. C., Magnetospheric convection and the high-latitude F2 ionosphere, *J. Geophys. Res.*, *79*, 1046, 1974.

Knudsen, W. C., P. M. Banks, J. D. Winningham, and D. M. Klumper, Numerical model of the convecting F2 ionosphere at high latitudes, *J. Geophys. Res.*, *82*, 4784, 1977.

Mendillo, M., J. Baumgardner, J. Aarons, J. Foster, and J. Klobuchar, Ground-based imaging of detailed arcs, ripples in the diffuse aurora, and patches of 6300 A emission, *Ann.Geophys.*, *5A*, 543, 1987.

Milan, S. E., T. K. Yeoman, M. Lester, E. C. Thomas, and T. B. Jones, Initial Backscatter occurrence statistics from the CUTLASSHF radars, *Ann. Geophys.*, *15*, 703, 1997.

Milan, S. E., M. Lester, S. W. H. Cowley, and M. Brittnacher, Convection and auroral response to a southward turning of the IMF:Polar UVI, CUTLASS, and IMAGE signatures of transient flux transfer at the magnetopause, *J. Geophys. Res.*, *105*, 15,741, 2000.

Namgaladze, A. A., O. V. Martynenko, A. N. Namgaladze, M. A. Volkov, Y. N. Korenkov, V. V. Klimenko, I. V. Karpov, and F. S. Bessarab, Numerical simulation of an ionospheric disturbance over EISCAT using a global ionospheric model, *J. Atmos. Terr. Phys.*, *58*, 297, 1996.

Providakes, J. F., M. C. Kelley, W. E. Swarts, M. Mendillo, and J. M. Holt, Radar and optical measurements of ionospheric process associated with intense subauroral electric fields, *J. Geophys. Res.*, *94*, 5350, 1989.

Rees, M. H., and J. C. G. Walker, Ion and electron heating by auroral electric fields, *Ann. Geophys.*, *24*, 193, 1968.

Rishbeth, H., and P. J. S. Williams, The EISCAT ionospheric radar: The system and its early results, *Q.J.R. Astron. Soc.*, *26*, 478, 1985.

Rodger, A. S., R. J. Moffett, and S. Quegan, The role of ion drift in the formation of ionization troughs in the mid- and high-latitude ionosphere—A review, *J. Atmos. Terr. Phys.*, *54*, 1, 1992.

Ruohoniemi, J. M., R. A. Greenwald, J.-P. Villain, K. B. Baker, P. T. Newell, and C.-I Meng, Coherent HF radar backscatter from small-scale irregularitiesin the dusk sector of the subauroral ionosphere, *J. Geophys. Res.*, *93*, 12,871, 1988.

Ruohoniemi, J. M., R. A. Greenwald, K. B. Baker, J.-P. Villain, C. Hanuise, and J. Kelly, Mapping high-latitude plasma convection with coherent HF radars, *J. Geophys. Res.*, *94*, 13,463, 1989.

Samson, J. C., D. D. Wallis, T. J. Hughes, F. Creutzberg, J. M. Ruohoniemi, and R. S. Greenwald, Substorm intensifications and field line resonances in the nightside magnetosphere, *J. Geophys. Res.*, *97*, 8495, 1992.

Schunk, R. W., and J. J. Sojka, Ion temperature variations in the daytime high-latitude F-region, *J. Geophys. Res.*, *87*, 5169, 1982.

Schunk, R. W., W. J. Raitt, and P. M. Banks, Effect of electric field on the daytime high-latitude E and F regions, *J. Geophys. Res.*, *80*, 3121, 1975.

Shand, B. A., M. Lester, and T. K. Yeoman, Substorm associated radar auroral surges: A statistical study and possible generation model, *Ann. Geophys.*, *16*, 441, 1998.

Smiddy, M., M. C. Kelley, W. Burke, F. Rich, R. Sagalyn, B. Shuman, R. Hays, and S. Lai, Intense poleward directed electric fields near the ionospheric projection of the plasmapause, *Geophys. Res. Lett.*, *4*, 543, 1977.

Sojka, J. J., R. W. Schunk, J. V. Evans, J. M. Holt, and R. H. Wand, Comparison of model high-latitude electron densities with Millstone Hill observations, *J. Geophys. Res.*, *88*, 77, 1983.

Sojka, J. J., R. W. Schunk, and J. A. Whalen, The longitude dependence of the dayside *F* region trough: A detailed model-observation comparison, *J. Geophys. Res.*, *95*, 15,275, 1990.

Southwood, D. J., and R. A. Wolf, An assessment of the role of precipitation in magnetospheric convection, *J. Geophys. Res.*, *83*, 5227, 1978.

Spiro, R. W., R. A. Heelis, and W. B. Hanson, Ion convection and the formation of the mid-latitude *F* region ionization trough, *J. Geophys. Res.*, *83*, 4255, 1978.

Spiro, R. W., R. A. Heelis, and W. B. Hanson, Rapid subauroral ion drifts observed by Atmospherics Explorer C, *Geophys. Res. Lett.*, *6*, 675, 1979.

Tsunoda, R. T., High-latitude *F* region irregularities: A review and synthesis, *Rev. Geophys.*, *26*, 719, 1988.

Whalen, J. A., Daytime F layer trough observed on a macroscopic scale, *J. Geophys. Res.*, *92*, 2571, 1987.

Whalen, J. A., The daytime *F* layer trough and its relation to ionospheric-magnetospheric convection, *J. Geophys. Res.*, *94*, 17,169, 1989.

Whalen, J. A., Properties of the F layer plasma in the midday throat ridge and trough, *Radio Sci.*, *29*, 219, 1994.

K. Hosokawa, Department of Geophysics, Graduate School of Science, Kyoto University, Kyoto, Japan. (hosokawa@kugi.kyoto-u.ac.jp)

T. Iyemori, Data Analysis Center for Geomagnetism and Space Magnetism, Graduate School of Science, Kyoto University, Kyoto, Japan. (iyemori@kugi.kyoto-u.ac.jp)

M. Lester, Department of Physics and Astronomy, University of Leicester, Leicester, U.K. (mle@ion.le.ac.uk)

N. Sato and A. S. Yukimatu, National Institute of Polar Research, Tokyo, Japan. (nsato@nipr.ac.jp; sessai@uap.nipr.ac.jp)

M. Sugino, Solar-Terrestrial Environment Laboratory, Nagoya University, Nagoya, Japan. (msugino@stelab.nagoya-u.ac.jp)

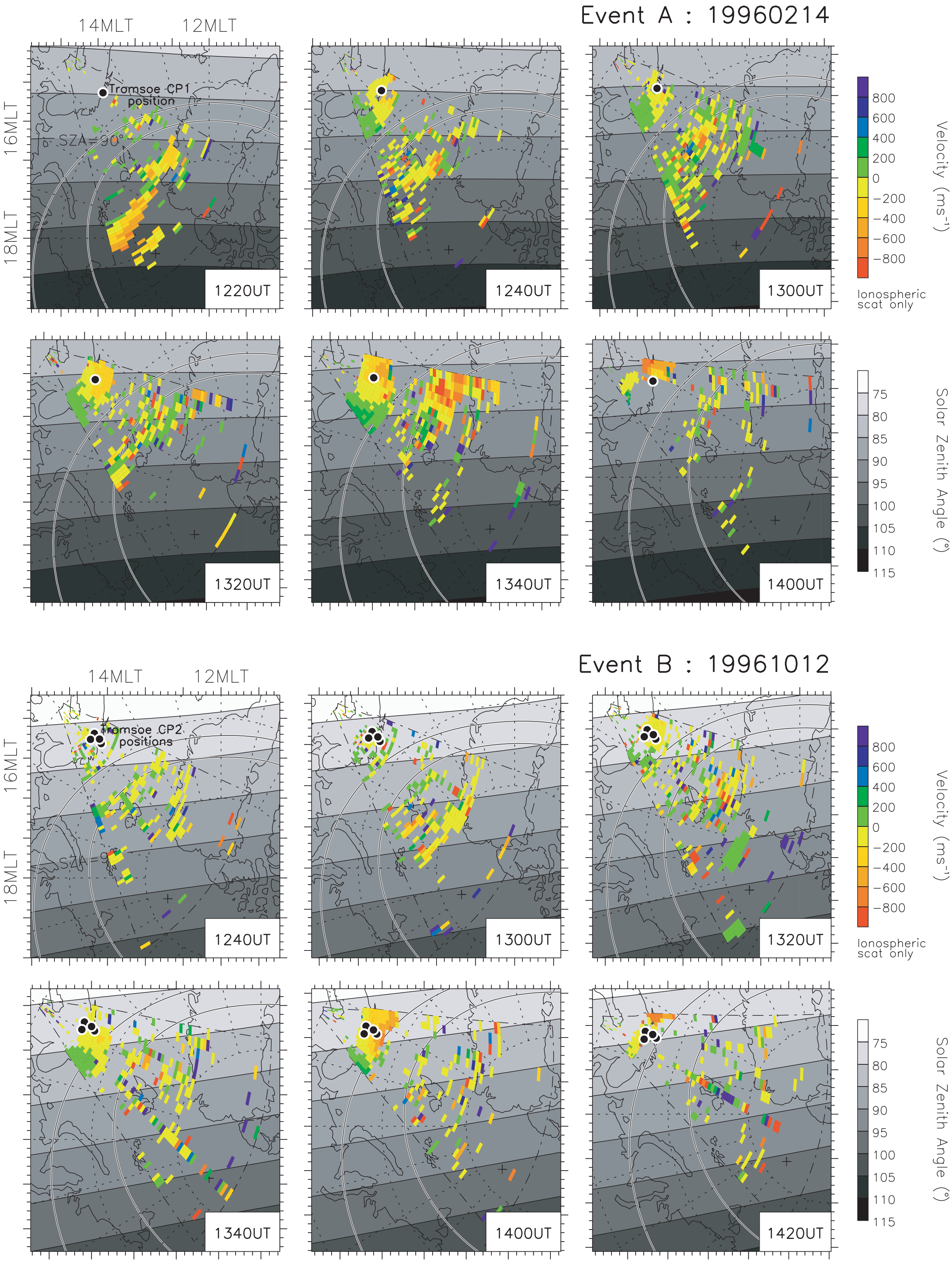
Event A : 19960214
14MLT
12MLT
16MLT
18MLT
Tromsoe CP1 position
SZA=90°
1220UT
1240UT
1300UT
1320UT
1340UT
1400UT
Velocity (ms⁻¹)
800
600
400
200
0
−200
−400
−600
−800
Ionospheric scat only
Solar Zenith Angle (°)
75
80
85
90
95
100
105
110
115
Event B : 19961012
14MLT
12MLT
16MLT
18MLT
Tromsoe CP2 positions
1240UT
1300UT
1320UT
1340UT
1400UT
1420UT

Figure 3. (opposite) Summary of the observation by the CUTLASS Finland radar for the two intervals of interest. The upper six panels show the set of the maps of the line-of-sight Doppler velocity illustrating development of the DUSE activity for event A (14 February 1996), and the lower six panels for event B (12 October1996), where motion of plasma away from the radar is negative, and toward the radar is positive. The poleward and equatorward edges of the Feldstein auroral oval [*Feldstein and Starkov*, 1967] as modeled by *Holzworth and Meng* [1975] are overplotted as Kp = 3 for event A and as Kp = 4 for event B. The background gray scaled colors display the contour of solar zenith angle.

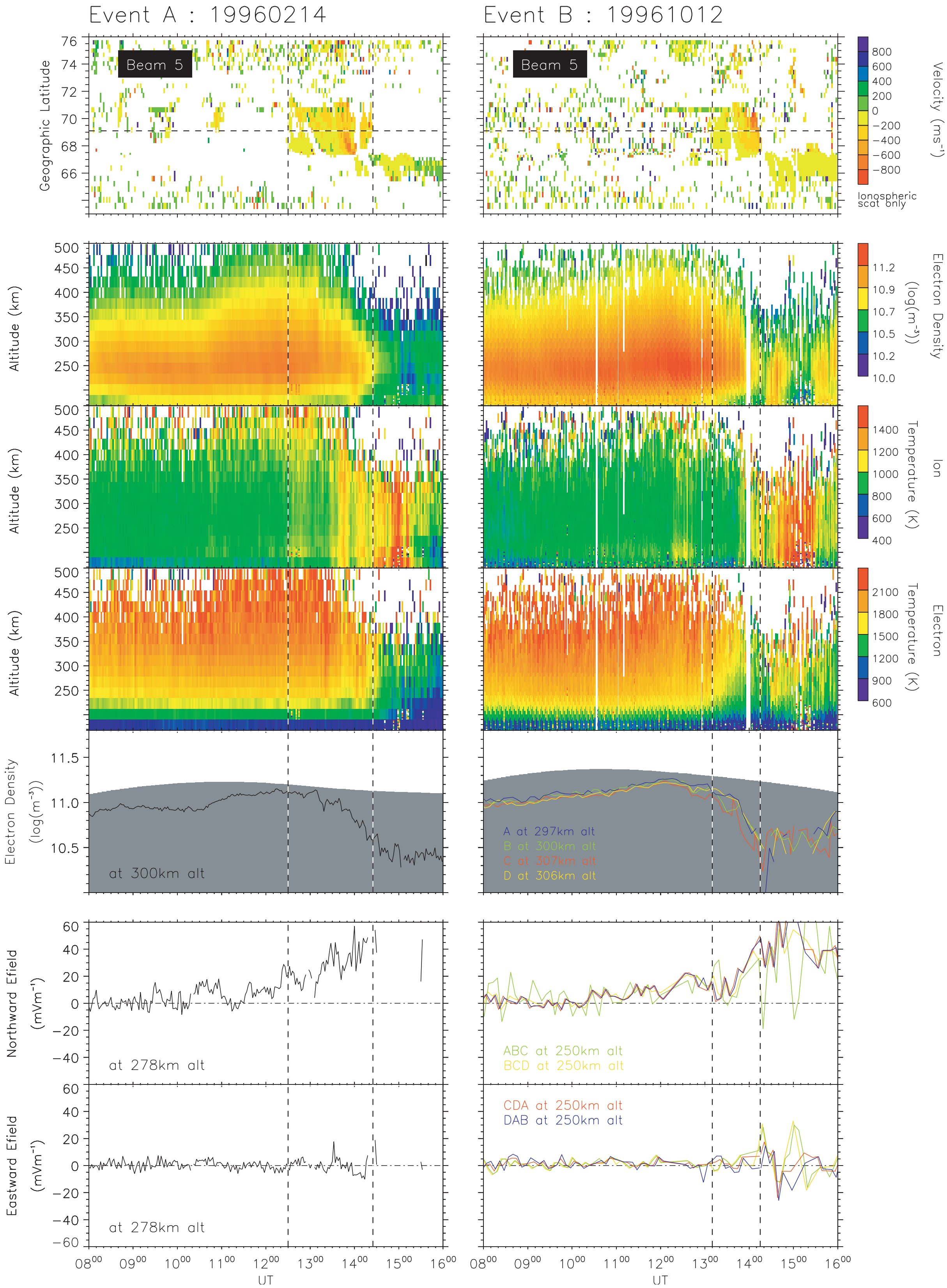
Event A : 19960214
Event B : 19961012
Beam 5
Beam 5
Geographic Latitude
Velocity (ms⁻¹)
Ionospheric scat only
Altitude (km)
Electron Density (log(m⁻³))
Ion Temperature (K)
Electron Temperature (K)
at 300km alt
A at 297km alt
B at 300km alt
C at 307km alt
D at 306km alt
Northward Efield (mVm⁻¹)
at 278km alt
ABC at 250km alt
BCD at 250km alt
Eastward Efield (mVm⁻¹)
CDA at 250km alt
DAB at 250km alt
at 278km alt
UT
UT

Figure 4. (opposite) Summary of the observations by the EISCAT UHF system for the two intervals of interest. The top two panels show the line-of-sight Doppler velocity observed by the CUTLASS Finland radar beam 5 from 0800 UT to 1600 UT on 14 February 1996 (left) and on 12 October 1996 (right). Horizontal dashed line indicates the latitude of gate 16 of Finland radar beam 5 which is a common volume with the EISCAT UHF system. Two vertical lines indicate duration of the DUSE for both events. Observations of the EISCATUHF system during both events are displayed in middle eight panels for event A (left) and for event B (right), where altitude profile of the electron density, ion temperature, electron temperature up to 500 km altitude, and electron density at 300 km altitude are shown. In the panel of electron density at 300 km altitude, electron density variation derived from IRI90 model is overplotted as a shadow. In the case of event B, observations of all four beams of the EISCAT CP-2 mode are plotted together. The bottom four panels indicate the geographic northward and eastward components of the electric field obtained from tristatic observation at 278 km altitude for event A (left) and determined from beam-swinging technique at 250 km altitude for event B(right).

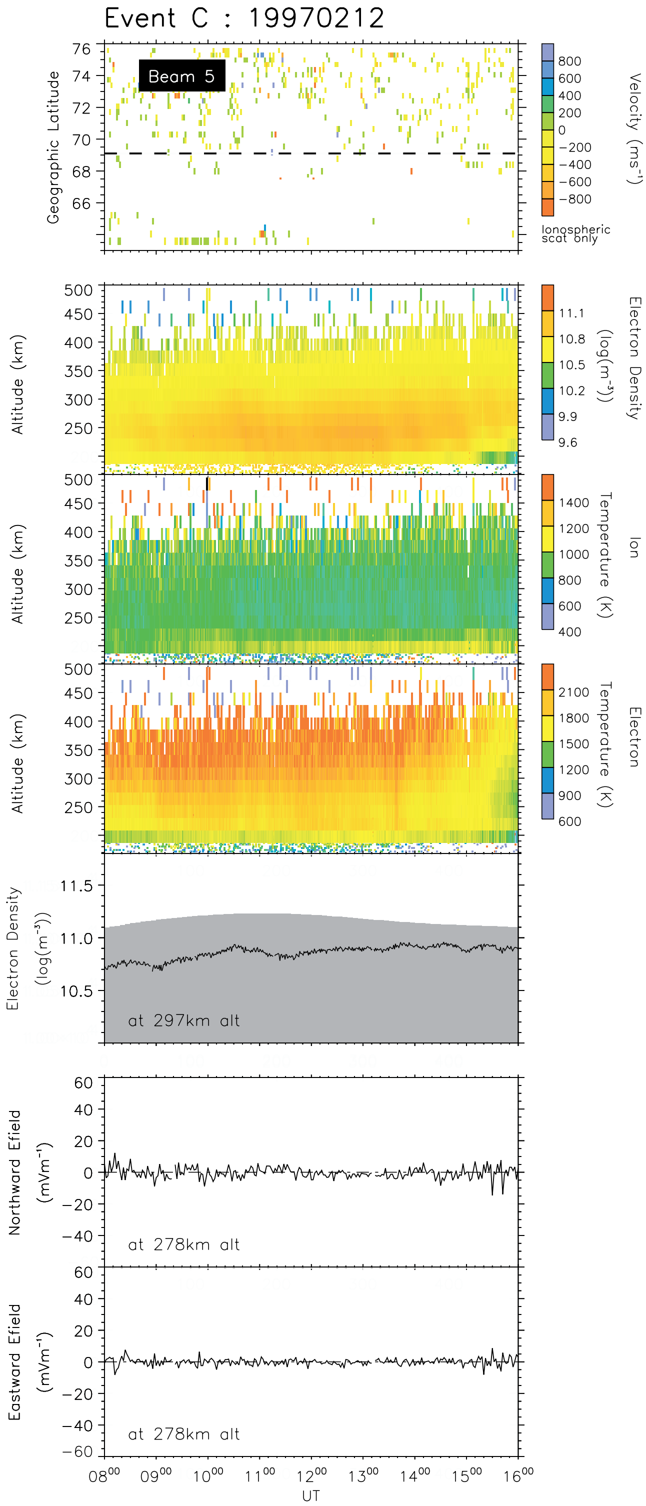

Figure 5. Summary of the observations from the CUTLASS Finland and the EISCAT UHF system for event C (12 February 1997), in which the DUSE was not observed by the CUTLASS Finland radar.

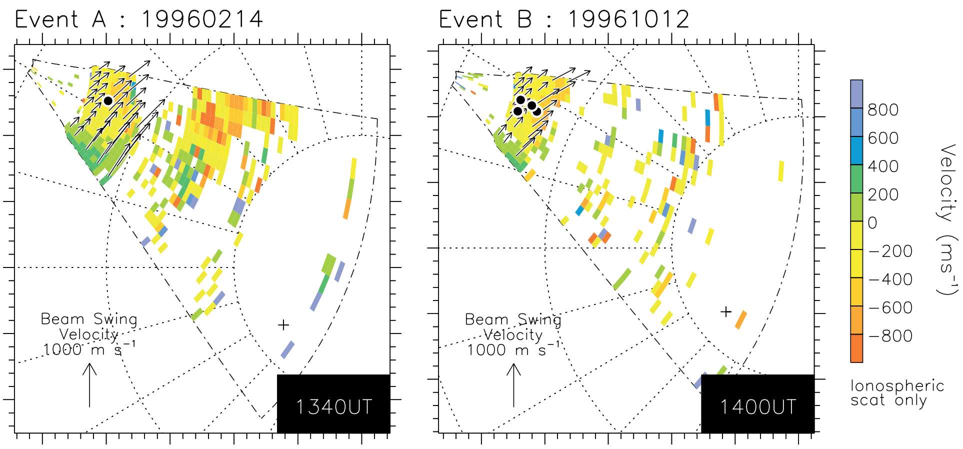

Figure 6. Line-of-sight Doppler velocity measurements from the CUTLASS Finland radar for selected scans of both intervals(1340 UT for event A and 1400 UT for event B, respectively),superimposed on which are two-dimensional velocity vectors estimated by applying a beam-swinging technique on the line-of-sight Doppler velocities.